

# CRAB CAVITIES FOR ILC

P. A. McIntosh<sup>†,1</sup>, STFC Daresbury Laboratory, Warrington, UK  
 S. Verdú-Andrés, B. Xiao, Brookhaven National Laboratory, Upton, NY, USA  
 R. Calaga, CERN, Geneva, Switzerland  
 S Belomestnykh, I. Gonin, S. Khabiboulline, A. Lunin, Y. Orlov, V. Yakovlev  
 Fermilab, Batavia, IL, USA  
 T. Okugi, A. Yamamoto, KEK, Tsukuba, Japan  
 G. Burt<sup>1</sup>, Lancaster University, Lancaster, UK  
 J. Delayen<sup>2</sup>, S. De Silva<sup>2</sup>, Old Dominion University, Norfolk, VA, USA  
<sup>1</sup>also at Cockcroft Institute, Warrington, UK  
<sup>2</sup>also at Jefferson Laboratory, Newport News, VA, USA

## Abstract

For the 14 mrad crossing angle proposed, crab cavity systems are fundamentally anticipated for the viable operation of the International Linear Collider (ILC), in order to maximise its luminosity performance. Since 2021, a specialist development team have been defining optimum crab cavity technologies which can fulfil the operational requirements for ILC, both for its baseline centre-of-mass energy of 250 GeV, but also extending those requirements out to higher beam collision intensities. Five design teams have established crab cavity technology solutions, which have the capability to also operate up to 1 TeV centre-of-mass. This presentation showcases the key performance capabilities of these designs and their associated benefits for both manufacture and integration into the ILC Interaction Point. The recommended outcome of the recently conducted crab cavity technology down-selection, will also be highlighted.

## INTRODUCTION

For the ILC's 14-mrad crossing angle, crab cavity systems are a fundamental priority from the reference ILC specifications for 250 GeV and scaling to 1 TeV operations [1] in order to maximise and maintain its luminosity performance. As part of a collective development programme, instigated by the ILC International Development Team (IDT) in 2018, the WP3 Crab Cavity consortium has devoted efforts to develop suitable technology solutions which will comply with ILC operational specifications.

From the associated beam delivery system (BDS) analysis, a minimum beam-pipe aperture of 25 mm is proposed, in order to comply with expected collimation provisions at the interaction point (IP). Figure 1 shows the practical space implementation and the associated cryomodule constraints, providing a longitudinal space availability of 3.85 m and a transverse beam-axis separation of 0.198 m, which dictates transversely, a highly compact ILC crab cavity (ILC-CC) structure design.

A total of five design solutions have been developed, each meeting the stringent specifications, which have been recently reviewed as part of a technology down-selection process. This first stage assessment has been to identify the 2 most effective designs, based on the respective E-M optimisations performed. Such a prioritised selection is also expected to facilitate early-stage procurement of niobium material (sheet or ingot) for the prototype cavity manufacture in conjunction with the associated HOM couplers, but explicitly excluding the forward power coupler (FPC). This prototype qualification will enable a second (and final) technology down-selection for the baseline ILC-CC technology, to be utilised primarily for the 125 GeV beam energy, but also ideally scalable for higher energies.

## ILC-CC DESIGN SPECIFICATIONS

The proposed ILC-CC RF parameters have been defined for 3 distinct operating frequencies; 1.3 GHz, 2.6 GHz and 3.9 GHz, thereby identifying the respective total kick voltages required for both operating energy requirements, including a 10 Hz RF repetition rate upgrade for the 250 GeV centre of mass option.

To assist in maximising the operational robustness and to reduce the anticipated breakdown-rate, conservative levels of maximum peak electric ( $E_p$ ) and peak magnetic ( $B_p$ ) fields have been adopted as 45 MV/m and 80 mT respectively. Table 1 shows the complete specifications for the ILC-CC system, which also identifies the dimensional space constraints, alignment tolerances, HOM impedance thresholds and kick factor requirements.

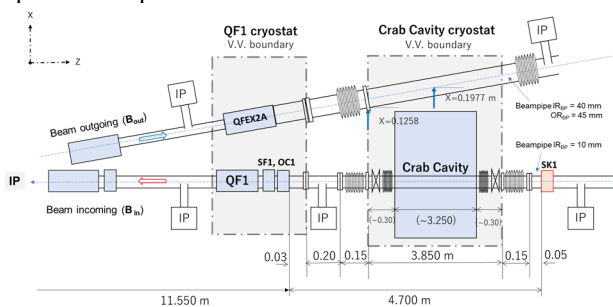


Figure 1: ILC crab cavity IP location.

<sup>†</sup> peter.mcintosh@stfc.ac.uk

Table 1: ILC-CC Specifications

| Parameter   | 250 GeV CoM   |       | 250 GeV CoM, 10 Hz Upgrade |     | 1 TeV CoM |           |
|---|---|-------|----------------------------|-----|-----------|-----------|
| Beam Energy (GeV) e-                                  | 125   |       |                            |     | 500       |           |
| Crossing Angle (mrad)                                 | 14  |       |                            |     |           |           |
| Installation site (m from IP)                         | 14  |       |                            |     |           |           |
| RF Repetition Rate (Hz)                               | 5   |       | 10                         |     | 4         |           |
| Number of bunches                                     | 1312  |       | 2625                       |     | 2450      |           |
| Bunch Train Length (ms)                               | 727   |       | 961                        |     | 897       |           |
| Bunch Spacing (ns)                                    | 554   |       | 366                        |     |           |           |
| Beam current (mA)                                     | 5.8   |       | 8.75                       |     | 7.6       |           |
| Operating Temp (K)                                    | 2   |       |                            |     |           |           |
| Cryomodule installation length (m)                    | 3.85 (incorporating gate valves)                          |       |                            |     |           |           |
| Horizontal beam-pipe separation (m)                   | 0.1967 (centre) ±0.0266 (each end of installation length) |       |                            |     |           |           |
| Cavity Frequency (GHz)                                | 3.9   | 2.6   | 1.3                        | 3.9 | 2.6       | 1.3       |
| Total Kick Voltage (MV)                               | 0.615   | 0.923 | 1.845                      | 2.5 | 3.7       | 7.4       |
| Max Ep (MV/m)   | 45  |       |                            |     |           |           |
| Max Bp (mT)   | 80  |       |                            |     |           |           |
| Amplitude regulation/cavity (% rms)                   | 3.5 (for 2% luminosity drop)                              |       |                            |     |           |           |
| Relative RF Phase Jitter (deg rms)                    | 0.069   |       |                            |     |           |           |
| Timing Jitter (fs rms)                                | 49 (for 2% luminosity drop)                               |       |                            |     |           |           |
| Max Detuning (kHz)                                    | 240   | 170   | 100 - 180                  | 240 | 170       | 100 - 180 |
| Longitudinal impedance threshold (Ohm)                | Cavity wakefield dependent                                |       |                            |     |           |           |
| Transverse impedance threshold (MOhm/m) (X, Y)        | 48.8, 61.7  |       |                            |     |           |           |
| Cavity field rotation tolerance/cavity (mrad rms)     | 5.2 (for 2% luminosity drop)                              |       |                            |     |           |           |
| Beam tilt tolerance (H and V) (mrad rms and μrad rms) | 0.35, 7.4 (for 2% luminosity drop)                        |       |                            |     |           |           |
| Minimum CC beam-pipe aperture size (mm)               | >25 (same as FD magnets)                                  |       |                            |     |           |           |
| Minimum Extraction beam-pipe aperture size (mm)       | 20  |       |                            |     |           |           |
| Beam size at CC location (X, Y, Z) (mm, μm, μm)       | 0.97, 66, 300   |       |                            |     |           |           |
| Beta function at CC location (X, Y) (m,m)             | 23200, 15400  |       |                            |     |           |           |
| Horizontal kick factor (kx) (V/pC/m)                  | $\ll 1.6 \times 10^3$                                     |       |                            |     |           |           |
| Vertical kick factor (ky) (V/pC/m)                    | $\ll 1.2 \times 10^2$                                     |       |                            |     |           |           |
| CC System operation                                   | assume CW-mode operation                                  |       |                            |     |           |           |

### 3.9 GHz RACETRACK

The original baseline ILC-CC for the ILC TDR [2] was a transversely compressed, 3.9 GHz elliptical cavity, made of 4 x 9-cell cavities for 1 TeV centre-of-mass (see Fig. 2).

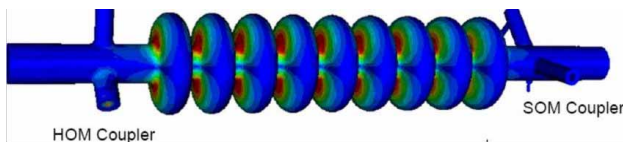


Figure 2: The original elliptical 3.9 GHz crab cavity developed for the ILC TDR.

In this latest specification iteration, the original design is not optimal, due to the higher 9-cell impedance. One of the major issues with the original design is the vertical dipole mode, or Same Order Mode (SOM), which is ~10 MHz from the crabbing mode and a redesign to separate the modes to use fewer cells is required. For dipole-mode cavities, the standard way to separate the two dipole polarisations is to use a racetrack cross-section, which has been developed by Lancaster University, UK.

Racetrack, elliptical and concave cross-section cavity geometries have been investigated with different aspect ratios. For each geometry, increasing the ratio of the major to minor axis pushes the SOM to higher frequencies, but unfortunately it also increases the lower order accelerating mode (LOM) in frequency, as well as bringing it closer to the crabbing mode and hence requires balancing.

The elliptical cross-section has a poorer mode separation than a racetrack cross section, due to the LOM moving more, while the concave geometry had higher Bp on the beampipe, hence the racetrack was chosen for further study. The optimum ratio of minor to major axis, having largest separation between the crab and its nearest mode, was 0.65 - 0.7, depending on the iris aperture. Racetrack geometries also alter Bp at the design gradient, decreasing it further to 0.55 - 0.6, after which it starts to increase as the walls come closer to the iris aperture (see Fig. 3). A 25 mm aperture with a 0.55 ratio of minor to major axis was chosen to minimize Bp while maximising the separation to the SOM which is the most dangerous unwanted mode.

Content from this work may be used under the terms of the CC BY 4.0 licence (© 2023). Any distribution of this work must maintain attribution to the author(s), title of the work, publisher, and DOI

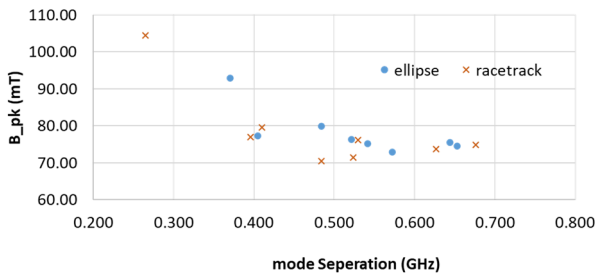


Figure 3: SOM frequency separation as function of Bp.

A downside of the racetrack geometry is that the cell-to-cell coupling is lower than a circular-cross section. An initial study of the LOM found that there was a high risk of trapped modes. A 3-cell racetrack structure was originally proposed, which whilst achieving ILC specifications, its operational margins could be improved further by adopting a 2-cell variant with larger apertures on the end groups (see Fig. 4), thereby providing stronger HOM damping.

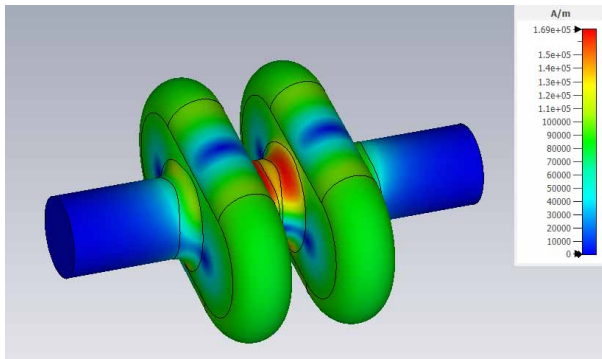


Figure 4: A 2-cell, 3.9 GHz racetrack carb cavity.

The 2-cell cavity needs to operate at 4 MV/m if we use 2 cavities for 125 GeV beam operation and the cavity operates with a Bp of 44.5 mT, meaning we have a 82% safety margin. The LOM passband is ~3.3 GHz and the SOM passband is ~4.7 GHz. A HOM coupler was designed to have strong damping peaks at both frequencies while having a notch filter at 3.9 GHz and mounted on either side of the cavity. The LOM impedance is only 400 kΩ and the highest transverse impedance is 3.75 MΩ/m. Other modes in the crabbing passband are <1 MΩ/m as the voltage in each cell cancel. No multipactor has been found near or below the operating voltage in CST, but some very high order resonant trajectories were found using SPARK3D. There is a resonant trajectory around 4 MV/m, but it is higher order and CST doesn't see any growth in secondaries. The first slow growth higher order multipactor is seen above the operating mode at 5.5 MV/m.

Simulations have been performed for the tuning sensitivity, Lorentz force and pressure detuning in CST mechanical solver. Tuning sensitivity is ~30 MHz/mm and pressure displacement at 1 bar is 2.1 mm, giving a 60 kHz frequency shift. Lorentz force is 1.0 kN/m<sup>2</sup> at 5 MV/m.

A conceptual cryostat design was also created to consider the length required in the beamline. A cryostat with a single cavity is 1.014 m long, while putting 4

cavities in a single cryostat would require 2.5 m, well within the 3.85 m space available.

### 1.3 GHz RF DIPOLE (RFD)

The RFD crab cavity is one of several crabbing cavities designed for ILC [2, 3]. Furthermore, the RFD cavity is also being implemented in both the LHC High Luminosity Upgrade [4] and Electron-Ion Collider [5] accelerators. The RFD design developed by Old Dominion University, USA in Fig. 5 operates in TE<sub>11</sub>-like mode where the major contribution to the transverse deflection is from the transverse electric field [6].

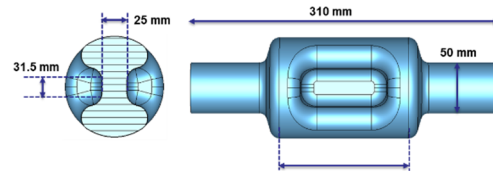


Figure 5: A 1.3 GHz RFD crab cavity.

The frequency of the RFD design is selected to be 1.3 GHz. 1-cell and 2-cell design options have been studied and the 1-cell structure has been selected for the baseline beam energy operation [7]. The RF properties of the 1.3 GHz RFD design is listed in Table 2, having no lower or SOM, with the pole shape being optimized to achieve maximum transverse voltage at the specified peak surface fields.

Table 2: RF Pproperties of the 1.3 GHz RFD Design

| Property              | 1-cell             | Unit           |
|-----------------------|--------------------|----------------|
| 1 <sup>st</sup> HOM   | 2.089              | GHz            |
| $E_p^*$               | 3.81               | MV/m           |
| $B_p^*$               | 6.78               | mT             |
| $[R/Q]_t (V^2/P)$     | 439.51             | Ω              |
| $G$                   | 129.88             | Ω              |
| $R_t R_s (V^2/P)$     | $5.71 \times 10^4$ | Ω <sup>2</sup> |
| $V_t$ per cavity      | 1.36               | MV             |
| $E_p$                 | 44.94              | MV/m           |
| $B_p$                 | 79.96              | mT             |
| At $E_t^* = 1.0$ MV/m |                    |                |

The RFD HOMs are damped using TESLA-style HOM couplers as shown in Fig. 6 [8].

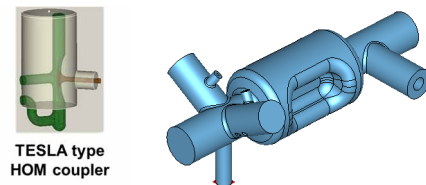


Figure 6: 1.3 GHz RFD crab cavity with two TESLA-type HOM couplers.

The transverse impedance *thresholds per cavity* for the 125 GeV (baseline) beam energy are  $Z_x \leq 24.4$  MΩ and  $Z_y \leq 30.85$  MΩ and for the 500 GeV (upgrade) beam energy are  $Z_x \leq 8.13$  MΩ and  $Z_y \leq 10.28$  MΩ. For both 125 GeV and 500 GeV beam operation, two TESLA-style couplers

are sufficient to suppress the longitudinal and transverse HOMs for both baseline and upgrade beam operations. The transverse impedance thresholds and impedances of the HOMs are shown in Fig. 7.

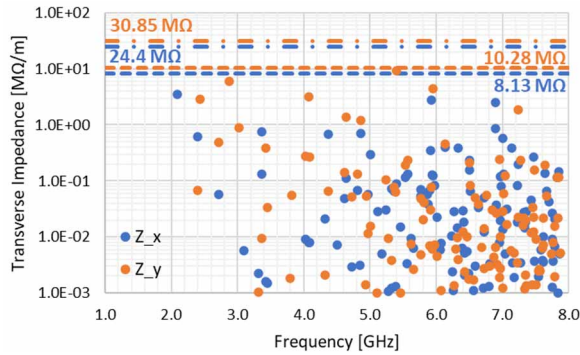


Figure 7: Transverse HOM impedances for a single 1.3 GHz RFD crab cavity.

The stresses for the 1.3 GHz RFD cavity with 3 mm thickness were analysed assuming room temperature Medium-Grain Nb material properties [9]. The resultant von-mises stress is 25 MPa which is significantly lower than the allowable stress of 39 MPa as shown in Fig. 8. This allows the cavity to be fabricated with variable thickness.

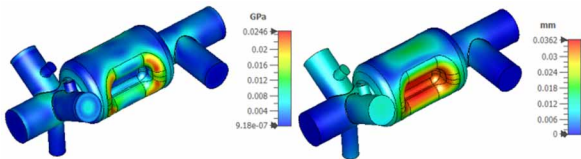


Figure 8: Von-Mises stress (left) and deformation (right) for the 1.3 GHz RFD crab cavity.

The RFD cavity will be fabricated following forming and machining techniques. The cavity components are shown in Fig. 9, with the end caps and centre body planned to be machined out of Medium Grain (MG) ingots.

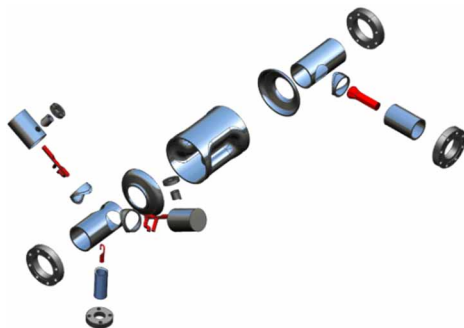


Figure 9: 1.3 GHz RFD cavity fabrication lay out.

### 1.3 GHz

### DOUBLE QUARTER WAVE (DQW)

A symmetric quarter wave deflecting DQW cavity at 400 MHz for crab crossing in the HL-LHC is already proposed, prototyped and successfully operated for the first demonstration of the crab crossing with proton beams in

the SPS of CERN [10, 11]. The ultra-compact geometry with an elliptical profile meets the tight transverse space constraints of the HL-LHC IP, while providing an excellent surface field to kick voltage ratio. A variation of the HL-LHC geometry was developed with a racetrack profile for the Electron-Ion Collider (EIC) purposes [12].

An oval cross section of the inductive part of cavity (shortened end of the poles) like the EIC design with a cavity waist similar to the HL-LHC design [9] resulted in a balanced peak surface fields for the cavity geometry at 1.3 GHz as developed by Brookhaven National Laboratory and CERN. This ultra-compact design is illustrated in Fig. 10 with the corresponding RF parameters in Table 3.

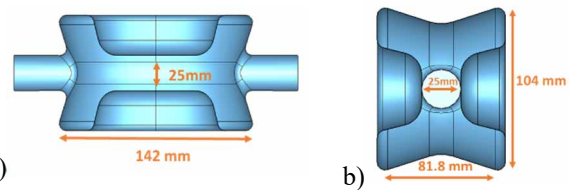


Figure 10: A 1.3 GHz, DQW crab cavity cross section a) longitudinal plane and b) horizontal plane.

With the specified peak surface fields, a total of 2 cavities are required to reach the 1.86 MV for the 125 GeV option while a 6 x DQW cavities will be required to reach the 7.4 MV needed for the 500 GeV option. The fundamental power required to generate this voltage is a moderate 300 W assuming a maximum beam offset of 1 mm and a pressure fluctuation of 50 Hz with a  $Q_L = 10^7$ . This coupling can be achieved with a hook type FPC similar to that of HL-LHC and adapting to the higher frequency.

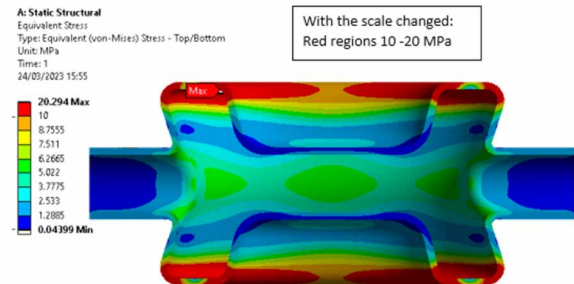


Figure 11: Nb sheet stress analysis (3 mm), fixed at the beam pipe extremities in the linear elastic analysis [13].

A preliminary stress analysis shows (see Fig. 11) that with 3 mm thick Niobium sheet and an external pressure of 1 bar, the peak stress is localized in the inductive regions and well below the maximum allowable stress.

Content from this work may be used under the terms of the CC BY 4.0 licence (© 2023). Any distribution of this work must maintain attribution to the author(s), title of the work, publisher, and DOI

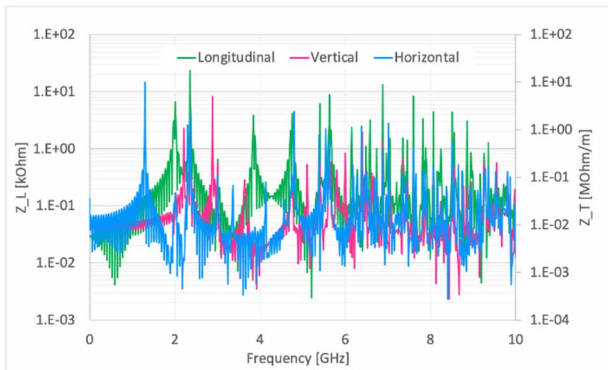


Figure 12: Impedance spectrum of the DQW bare cavity.

All other HOMs are situated above the fundamental 1.3 GHz frequency, with a very large separation (> 2 GHz). This lends itself to a simpler damping scheme without affecting the crabbing mode. The impedance spectrum of the longitudinal and transverse modes is shown in Fig. 12.

A first study with two TESLA-type HOM dampers on the inductive part of the cavity already brings all modes to within the specification (Table 3).

Table 3: RF Parameters

| Parameter             | unit      | value           |
|-----------------------|-----------|-----------------|
| Frequency             | [GHz]     | 1.3             |
| First Long HOM        | [GHz]     | 2.0             |
| First Tran HOM        | [GHz]     | 2.21            |
| Ep/Et                 |           | 3.6             |
| Bp/Et                 | [mT/MV/m] | 6.14            |
| Rt/Q                  | [Ω]       | 422             |
| Cavity diameter       | [mm]      | 104             |
| Aperture              | [mm]      | 25              |
| Cavity Q <sub>L</sub> |           | 10 <sup>7</sup> |
| Input Power           | [kW]      | 0.3             |
| Stored Energy         | [J]       | 0.25            |
| Nb per cavity         | [kg]      | ~15             |

HL-LHC type coaxial couplers can be used if stronger damping is required to ease its mountability. Due to very high frequency of the HOMs and the small size, a waveguide damping scheme could prove to be an interesting option and is under investigation (see Fig. 13).

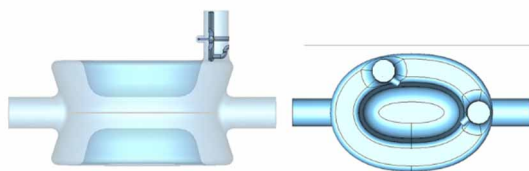


Figure 13: Coaxial damping with ILC type couplers.

Due to the available space of 3.85 m in the ILC IR, a first integration analysis was carried out. It shows the feasibility of 6 x DQW cavities in a single cryostat can functionally comply (see Fig. 14). However, a detailed integration study is required to understand realistic cold-to-warm transitions and gate valve constraints to be able identify any issues.

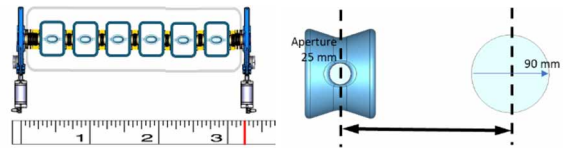


Figure 14: Preliminary integration in a cryomodule (left) and the cavity to adjacent beam pipe separation (right).

### 1.3 GHz WIDE OPEN WAVEGUIDE (WOW)

For a Wide-Open-Waveguide (WOW) cavity design, the fundamental mode is trapped in the cavity, LOMs should not exist and all and all other HOMs leak out through the beampipe and get absorbed. For the WOW cavity, an RFD structure is used [7], with a 100 mm inner diameter beampipe to allow propagation of the lowest frequency longitudinal and transverse HOMs. The optimized cavity geometry as developed by Brookhaven National Laboratory is shown in Fig. 15, which is expected to reach 1.6 MV/cavity.

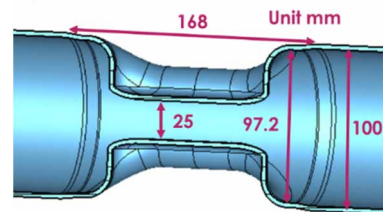


Figure 15: The bare 1.3 GHz WOW crab cavity.

The major benefit of a WOW-type design is that the HOM damper is decoupled from the bare cavity design. It is outside the helium vessel which simplifies the fabrication while comparing with LHC or EIC designs [14]. The fundamental mode is attenuated to a level that is low enough on the HOM damper so that it is multipacting free.

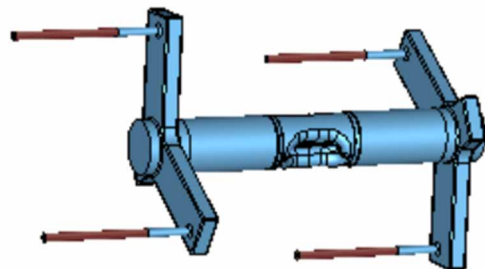


Figure 16: Cu waveguide-coax damper for WOW cavity.

To fulfill the space requirement, 2 adjacent cavities share the damper unit in-between, with 2 additional dampers on each end (see Fig. 16).

Cu waveguide-coax damper units is proposed, the fundamental mode attenuates in the waveguide in the transverse plane, thus it can be made compact longitudinally. The HOM power is not a concern since ILC is a mA range pulsed machine. The calculated impedance spectrum of this design is well within budget, as shown in Fig. 17.

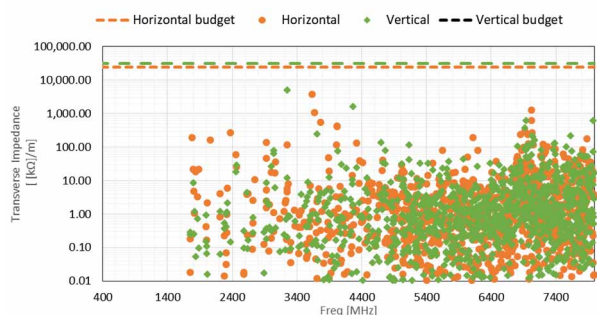


Figure 17: Transverse impedance of the WOW type cavity with Cu waveguide to coax damper.

Multipacting simulations were performed for the bare cavity and HOM damper unit, which as expected showed no multipacting and behaves similarly to the LHC and EIC RFD without end-groups. It is proposed to use the LHC RFD-type scissor jack tuner that applies force symmetrically in a vertical direction to the top and bottom of the cavity. Simulations show that the bare cavity with 3 mm thick Nb produces a maximum 28 MPa stress under 2.2 atm external pressure at room temperature. At 2 K, with 2.5 kN force on each side, the maximum stress on the bare cavity is 0.24 GPa with 0.12 mm displacement on each side. With a 10.2 MHz/mm tuning sensitivity, the tuning range is 2.5 MHz. For 180 kHz tuning requirement, 370 N force with 18  $\mu$ m displacement would suffice. The pressure sensitivity is 725 Hz/mBar for a bare cavity and 308 MHz/mBar with the tuner fixed. The Lorentz force detuning is  $-1.51 \text{ kHz/MV}^2$ , which is  $-3.31 \text{ kHz}$  for 1.48 MV, which can be compensated by the tuner. The helium vessel would help stiffen the cavity towards better mechanical performance. Top plot in Fig. 18 shows the cryomodule with 5 WOW cavities and 6 damper units, which can be fitted into the 3.85 m space.

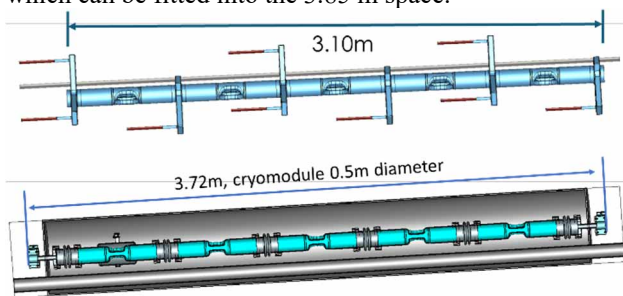


Figure 18: Cryomodule WOW cavity string assembly with waveguide-coax (top) and simplified stainless steel beampipe dampers (bottom).

A simplified design, using stainless steel bellows as the damper unit has also been proposed, see bottom plot in Fig. 18. Since HOMs propagate along the beampipe, for HOMs this design is one multi-cell cavity with both superconducting Nb and normal conducting stainless steel as cavity wall. Simulations reveal that this design also meets the impedance budget.

## 2.6 GHz QUASI-WAVEGUIDE MULTICELL RESONATOR (QMIR)

A final ILC-CC design option proposed by Fermilab is a novel Quasi-waveguide Multicell Resonator (QMIR) originally developed for Short Pulse X-Ray operation of the ANL APS Upgrade project [15]. The cavity is fully open at both ends and connected to the beam vacuum chamber. Proposed solution significantly reduces the loaded quality factor of trapped HOMs, eliminates the need of dedicated HOM couplers, and thus simplifies the mechanical design of the cavity. A prototype QMIR deflecting cavity was built and successfully tested at 2 K in a vertical Test Stand (VTS), demonstrating a record transverse kick of 2.6 MV [16]. We redesigned the cavity shape and increased the aperture to 25 mm to meet the requirements for the ILC crab cavity [17]. The cavity frequency was chosen to be 2.6 GHz, the linac operating mode second harmonic, as good compromise to provide the necessary kick and fit into the available transverse and longitudinal installation space. For this frequency the total kick is to be 0.92 MV for 125 GeV beam and 3.7 MV for 500 GeV beam, respectively.

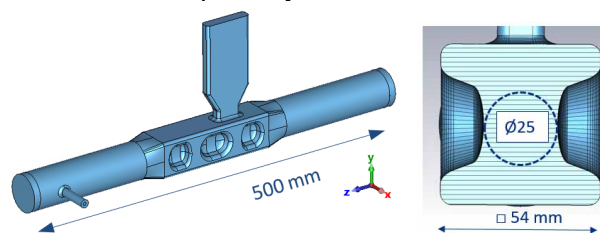


Figure 19: The 2.6 GHz QMIR crab cavity.

The cavity geometry with overall dimensions is illustrated in Fig. 19, where three pairs of electrodes form a deflecting trapped dipole  $\pi$ -mode used in crab cavity operation. A single waveguide port is used to feed RF power to the operating mode and also to extract the SOM power.

The wakefield excitation in the cavity has been simulated and analysed, it completely satisfies the cavity requirement. Resonance HOM excitation has been investigated also, using probabilistic model [18]. The probability that a single HOM is in resonance with the beam harmonic depends on the statistical spread of HOM parameters, frequencies, Q-factors and impedances. To estimate this probability, 100k cavities have been calculated with a normal deviation of HOM frequencies which are determined in turn by expected fabrication imperfectness. Based on the simulation data, the HOM power radiating through the cavity ports will not exceed 1.7 W. The estimated budget for the cavity cryogenic losses ( $<2.7 \text{ W}$ ) and RF input power requirements ( $<1.5 \text{ kW}$ ) appear operationally feasible.

To verify the cavity tunability and tuning range, electromechanical analysis of a bare cavity using COMSOL software [19] was performed. The dependences of the LFD coefficient and pressure variation ( $dF/dP$ ) on the cavity wall thickness are shown in Fig. 20.

Content from this work may be used under the terms of the CC BY 4.0 licence (© 2023). Any distribution of this work must maintain attribution to the author(s), title of the work, publisher, and DOI

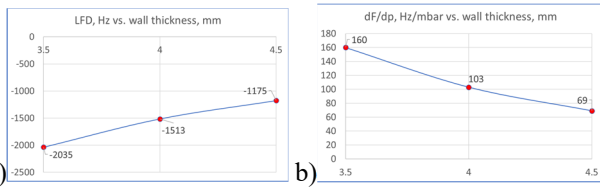


Figure 20: a) Calculated LFD coefficients and b) dF/dP of QMiR cavity with different wall thicknesses.

Both coefficients LFD and dF/dP are smaller than the cavity bandwidth, noting that the LFD can be further reduced by adding stiffeners to the design, making it potentially possible for the QMiR crab cavity to operate without a fast frequency tuner.

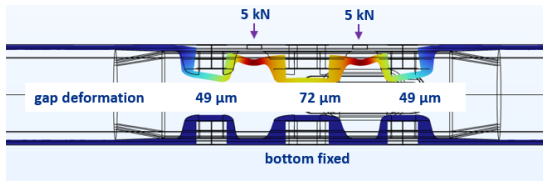


Figure 21: Mechanical analysis of the frequency tuning range in the QMiR cavity with 4 mm wall thickness.

The deformation of the cavity walls was simulated for applied fixed external forces of 10 kN, uniformly distributed over two contact pads, as shown in Fig. 21 for a wall thickness of 4 mm. The found cavity sensitivities to frequency tuning and to external forces are -35 kHz/μm and -190 kHz/kN, respectively. This allows to have a frequency tuning range of up to 2 MHz. The cavity mechanical design including a LHe vessel, a compact frequency tuner and a cryomodule concept has been developed. The entire Crab Cavity cryomodule design is shown in Fig. 22.

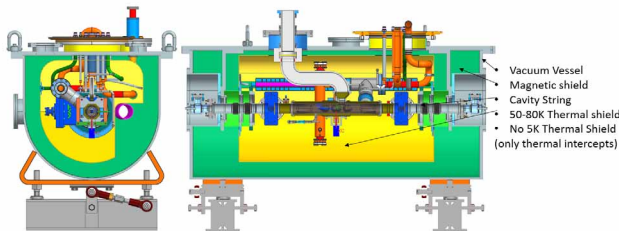


Figure 22: The cryomodule concept design.

The cryomodule fits ILC technical requirements and environment limitations. Internal alignment system and oversized backward beam pipe allow external adjustment of the cavity position ( $\pm 0.1$  mm). Design of the vacuum vessel and piping satisfies the safety codes. The near-term plan is to complete mechanical design of the cavity, manufacture, process and test it at high gradient at the Fermilab VTS.

### THE ILC-CC DOWN-SELECTION

Over the period 4<sup>th</sup> – 6<sup>th</sup> April 2023, a technology down-selection review was undertaken at KEK, Tsukuba, Japan. The review panel chair, Dr. Bob Laxdal (TRIUMF), along with appointed independent SRF specialists; Eiji Kako and Hiroshi Sakai (KEK), Enrico Cenni (CEA), Michele

Bertucci (INFN) and Rong-Li Geng (ORNL), along with BDS specialist Toshiyuki Okugi (KEK), found that there were no show-stoppers for any of the cavity designs. All had the potential to appropriately comply with the 250 GeV and to 500 GeV within the specified specifications, each also had scalability to 1 TeV centre-of-mass operation. Some designs were more advanced than others and some had more operational margin.

A weighted collective assessment was conducted on the basis of; specification compliance, cavity design, prototype development, HOM analysis/mitigation, RF ancillaries FPC/tuners, multipactor, df/dP, cavity tuning, fabrication, cryomodule implications, compliance for ILC500 and overall risk. The conclusion to propose the 2 most optimum designs to be subsequently prototyped are:

- 1.3 GHz, RF Dipole, Old Dominion University
- 2.6 GHz, QMiR, FNAL

As a result of this decision, both design teams are currently in close discussions with KEK to pursue early-stage procurement of the required niobium material (sheet or ingot) to facilitate prototype manufacture of a single unjacketed cavity and its associated HOM couplers but excluding the forward power coupler. Once manufactured, it is anticipated that each design is then tested in terms of cold RF performance and HOM characteristics.

### NIObIUM MATERIAL EXPECTATIONS

SRF accelerator applications demand high performance and cost effective SRF accelerator technology. Fine-grain (FG) and large-grain (LG) niobium (Nb) SRF cavity production have matured and been applied in various projects and research programs. Medium-grain (MG) Nb material has been recently developed and demonstrated as cost effective Nb ingot production and/or disc production by directly slicing discs from a forged and annealed Nb ingot [20 - 23]. Table 4 gives a summary of their production process and features.

Table 4: Summary of Niobium Production Processes

|   | FG (sheet)   | MG (disc)                             | LG (disc)   |
|---|--|---------------------------------------|---|
| Process started with                        | Forged to block, rolled, and grinded               | Forged to smaller cylinder and sliced | Directly sliced   |
| Cleanliness                                 | Prone to contamination due to rolling and grinding | Clean surface with directly sliced    | Clean surface best proven with no-forging and directly sliced |
| Grain size grade (ASTM) Physical grain size | 5 ~ 6<br>< 0.1 mm                                  | 0 ~ 3<br>< 1 mm                       | n/a<br>> 10 mm  |
| Mechanical property                         | Very uniform                                       | Reasonably uniform                    | Non uniform, depending on the                                 |

|                 |           |                |                     |
|-----------------|-----------|----------------|---------------------|
|                 |           |                | crystal orientation |
| Production cost | Expensive | Less expensive | Least expensive     |

Both LG and MG Nb material provides advantages of (i) surface cleanliness without rolling process for sheet production which is inevitable for FG material and (ii) cost saving for direct slicing, eliminating the rolling process.

Table 5: MG Nb Material Produced by ATI

| Chemical Composition (%) | Other Properties                           |
|--------------------------|--|
| Ta: <0.01                | Dims: 260 mm (dia), 2.8 mm (t)             |
| W: <0.003                | RRR: >450                                  |
| Ti, Si, Mo, Fe: <0.003   | Recrystallisation: 100%                    |
| Ni: <0.002               | Grain sz: 0.2~0.3 mm (ASTM: 1~2)           |
| H2: <0.003               | Hardness (HV0.1): 40~44                    |
| C: <0.002                | Mechanical Strength:                       |
| N2: <0.002               | Ult Strgth (RT): 141–146 Nmm <sup>-2</sup> |
| N2: <0.002               | Yield Strgth (RT): 56–61 Nmm <sup>-2</sup> |

However there has been an issue of mechanical characteristics for LG because of non-uniform mechanical property, depending on the random grain orientation/direction. The MG ingot/disc provides reasonably uniform and stable mechanical property because of sufficiently smaller grain size (< 1 mm) compared with the cavity structure scale (~ 10 cm). A recent development effort in cooperation between KEK, JLab, and ATI, multiple MG Nb ingots have been successfully developed, as summarized in Table 5.

Based on this progress, one of the down-selected proposals, RFD, for the crab cavity prototype development, has proposed a fabrication of the prototype cavity with mechanical machining by using MG Nb material (ingot). The other prioritised QMIR proposal, may be also be fabricated using direct machining. In this case, heavy forging will be required, and FG Nb material may need to be considered.

## CONCLUSIONS

The ILC-CC development as part of the ILC IDT WP3 programme, has arrived at two most optimum crab cavity technology solutions, which will now be taken forward to a prototype and validation stage. All five original technology solutions, operating over a broad range of RF frequencies, were identified to be compliant with ILC specifications by a specialist review panel, who have subsequently selected the RFD and QMiR crab cavity designs to be taken forward to the next stage of development.

## ACKNOWLEDGEMENTS

The author would like to specifically recognise the valuable guidance and support from the ILC IDT WP1/WP2 Coordinator Kirk Yamamoto (KEK) and ILC IDT Coordinator Shin Michizono (KEK) for all WP3 development activities for ILC to date and for hosting the down-selection review at KEK.

## REFERENCES

- [1] European Strategy for Particle Physics Preparatory Group, “Physics Briefing Book”, arXiv, Jan. 2020. doi:10.48550/arXiv.1910.11775
- [2] C. Adolphsen *et al.*, “The International Linear Collider Technical Design Report-Volume 3.I: Accelerator R&D in the Technical Design Phase”, arXiv, 2013. doi: 10.48550/ arxiv.1306.6353
- [3] C. Adolphsen *et al.*, “The International Linear Collider Technical Design Report - Volume 3.II: Accelerator Baseline Design”, arXiv, 2013. doi:10.48550/arxiv.1306.6328
- [4] R. Calaga, “Crab Cavities for the High-Luminosity LHC”, in *Proc. SRF’17*, Jul. 2017, pp. 695-699. doi:10.18429/JACoW-SRF2017-THXA03
- [5] S. U. De Silva *et al.*, “197 MHz Waveguide Loaded Crabbing Cavity Design for the Electron-Ion Collider”, in *Proc. NAPAC’22*, Albuquerque, NM, USA, August 2022. doi:10.18429/JACoW-NAPAC2022-WEPA26
- [6] S. U. De Silva and J. R. Delaysen, “Cryogenic Test of a Proof-of-principle Superconducting RF-Dipole Deflecting and Crabbing Cavity”, *Phys. Rev. Accel. Beams*, vol. 16, p. 082001, 2013.
- [7] S. U. De Silva *et al.*, “Design of a 1.3 GHz RF-Dipole Crabbing Cavity for International Linear Collider”, in *Proc. LINAC’22*, Liverpool, UK, Aug-Sep 2022, pp. 832 – 834.
- [8] P. Kneisel and J. Sekutowicz, “Update on coaxial coupling scheme for International Linear Collider-type cavities”, *Phys. Rev. Accel. Beams*, vol. 13, p. 022001, 2010. doi:10.1103/PhysRevSTAB.13.022001
- [9] A. Yamamoto, “New Nb Material for Cost Saving”, International Workshop on Future Linear Colliders ((LCWS2023), SLAC National Accelerator Laboratory, May 2023.
- [10] R. Calaga, S. Belomestnykh, I. Ben-Zvi, J. Skaritka, Q. Wu, and B. P. Xiao, “A Double Quarter Wave deflecting cavity for the LHC”, in *Proc. IPAC’13*, Shanghai, China, May 2013, paper WEPWO047, pp. 2408-2410.
- [11] R. Calaga *et al.*, “First demonstration of the use of crab cavities on hadron beams”, *Phys. Rev. Accel. Beams*, vol. 24, p. 062001, Jun. 2021. doi:10.1103/PhysRevAccelBeams.24.062001
- [12] S. Verdú-Andrés and B. P. Xiao, “Pathways for a compact double-quarter wave cavity with low peak surface fields and large deflecting kick”, BNL Technical Note EIC-ADD-TN-024, Sep. 2021.
- [13] J. Swieszek *et al.*, private communication, 2023.
- [14] B. Xiao *et al.*, “HOM Damper Design for BNL EIC 197 MHz Crab Cavity”, in *Proc. SRF’21*, East Lansing, MI, USA, Jun.-Jul. 2021, pp. 624. doi:10.18429/JACoW-SRF2021-WEPCAV014
- [15] A. Lunin, I. Gonin, M. Awida, T. Khabiboulline, V. Yakovlev, and A. Zholents, “Design of a Quasi-waveguide Multicell Deflecting Cavity for the Advanced Photon Source”, *Phys. Procedia*, vol. 79, pp. 54-62, 2015. doi:10.1016/j.phpro.2015.11.062
- [16] Z. Conway *et al.*, “Development and Test Results of a Quasi-waveguide Multicell Resonator”, in *Proc. IPAC’14*, Dresden, Germany, Jun. 2014, pp. 2595-2597. doi:10.18429/JACoW-IPAC2014-WEPRI050



Content from this work may be used under the terms of the CC BY 4.0 licence (© 2023). Any distribution of this work must maintain attribution to the author(s), title of the work, publisher, and DOI

- [17] A. Lunin *et al.*, “Compact Multicell Superconducting Crab Cavity for ILC”, presented at SRF’23, MI, USA, Jun. 2023, paper TUPTB044, this conference.
- [18] A. Lunin, T. N. Khabiboulline, N. Solyak, A. I. Sukhanov, and V. P. Yakovlev, “Statistical Analysis of the Eigenmode Spectrum in the SRF Cavities with Mechanical Imperfections”, in *Proc. ICAP’18*, Key West, Florida, USA, Oct. 2018, pp. 265-269.  
doi:10.18429/JACoW-ICAP2018-TUPAG04
- [19] <https://www.comsol.com>
- [20] A. Yamamoto *et al.*, “Ingot Nb based SRF Technology for the International Linear Collider”, *AIP Conf. Proc.*, vol. 1687, p. 030005, Dec. 2015. doi:10.1063/1.4935326
- [21] A. Kumar *et al.*, “Mechanical Properties of Directly Sliced Medium Grain Niobium for 1.3 GHz SRF Cavity”, in *Proc. SRF’21*, East Lansing, MI, USA, Jun.-Jul. 2021, pp. 259.  
doi:10.18429/JACoW-SRF2021-MOPCAV004
- [22] T. Dohmae *et al.*, “Fabrication of 1.3 GHz SRF Cavities Using Medium Grain Niobium Discs Directly Sliced from Forged Ingot”, in *Proc. SRF’21*, East Lansing, MI, USA, Jun.-Jul. 2021, pp. 287.  
doi:10.18429/JACoW-SRF2021-MOPCAV012
- [23] G. Myneni *et al.*, “Medium Grain Niobium SRF Cavity Production Technology for Science Frontiers and Accelerator Applications”, *J. Instrum.*, vol. 18, p. T04005, Apr. 2023.  
doi:10.1088/1748-0221/18/04/T04005